Energy and Exergy Analysis of a HVAC System Having a Ground Source Heat Pump as Generation System

Paolo Valdiserri – University of Bologna, Italy – paolo.valdiserri@unibo.it
Michael Lucchi – University of Bologna, Italy – michael.lucchi2@unibo.it
Marco Lorenzini – University of Bologna, Italy – marco.lorenzini@unibo.it

Abstract

This study reports on a dynamic simulation of the annual performance of a HVAC system consisting of a ground coupled heat pump (GCHP), which has which has a ground heat exchanger with horizontal pipes for winter and summer seasons. The simulations are performed by employing the software Trnsys. The HVAC system is connected to a thermal storage tank containing warm water in winter and cold water in summer, which serves a single-family dwelling located in the city of Rome, Italy. A first- and second-law analysis of the yearly performance of the entire system and of the single components was carried out, highlighting the components with the lowest exergy efficiency.

1. Introduction

In the European Union, the energy consumption in the building sector has reached 40% of yearly energy demand and contributes to around 36% of CO_2 emissions. To reduce these figures, EU member States are required to take actions that are compliant with the Energy Performance of Buildings Directive. Different strategies have been adopted by the single member states to reduce this energy consumption and to improve the energy efficiency in buildings. Among these are increasing the insulation thickness of the building envelope (Loreti et al., 2016), employing more efficient HVAC systems and using renewable energies (Valdiserri, 2018).

As far as the use of renewables are concerned, it is worth mentioning that in 2009 and 2018 the European Parliament identified aero-thermal, geothermal and hydrothermal energy as renewable energy source (RES). Ground-coupled heat pump (GCHP) systems for heating and cooling of new and existing buildings satisfy both the demand of primary energy saving and the goal of the directive on renewable energy. As the soil can provide a higher temperature for heating and a lower temperature for cooling than the external air does, ground-coupled heat pumps usually reach higher COPs and EERs than those using outdoor air as a heat reservoir. Vertical and horizontal ground heat exchangers (Sarbu and Sebarchievici, 2014), GHEs, are usually connected with heat pumps: the single-pipe horizontal configuration is the easiest and cheapest to install, although it requires that a large plot of land be available close to the building served. Horizontal GHEs consist of a series of parallel pipe arrangements laid out in trenches dug approximately 1-2 metres below ground surface (Sanaye and Niroomand, 2010). Due to the low installation depth, horizontal GHEs are more affected by ambient temperature variations than vertical probes, so they require a more accurate design (Lucchi et al., 2017).

All the studies cited above focus on quantitative energy consumption without accounting for its quality. This is only possible through a second law approach, which can be implemented through an exergy analysis. Several studies suggest that the combination of low-temperature heating systems, with low-exergy sources, such as GCHP (e.g. Evola et al., 2018) are a profitable strategy for energy saving in buildings. In order to carry out an appropriate exergy analysis of an unsteady energy process, the definition of a dead state is of paramount importance. In cases such as the one studied here, where outdoor thermodynamic variables (temperature in particular) change over the day and over the seasons, there is no definition agreed upon by the whole scientific community (Serova and Brodianski,

2004). Some authors use the average outdoor temperature in the heating and cooling seasons as the reference temperature, whilst others (Zhou and Gong, 2013) calculated the exergy flow rate considering as dead state the hourly outdoor temperature. In this study the latter approach, i.e. a time-dependent dead state temperature, was adopted, as discussed below.

The aim of this work is to numerically evaluate the performance of a HVAC system consisting of a ground-coupled heat pump (GCHP) with horizontal GHE and both hot- and cold-water storage tanks for year-round operation. Simulations were run for a typical year for a single-family detached house around Rome, Italy. Data are presented on a monthly basis and for the whole year. The model was developed in the dynamic environment of Trnsys® 17 Simulation Studio (Klein et al., 2017). The energy analysis was conducted both in terms of first and second law of thermodynamics and the results for a typical year are discussed.

2. The Case Investigated

The building chosen for the simulation is a detached house located in Rome. It is a two-storied building with only the ground floor conditioned, with a living room, a kitchen, two bedrooms and a bathroom. The building was set-up in Sketchup® (Fig. 1).

The net surface area is 68.0 m^2, whereas the total area, including walls is 83.4 m^2. The net volume of the house to be conditioned is 183.8 m^3, and the envelope through which heat is exchanged with the ambient is 276.6 m^2. In terms of the thermal characteristics of the building envelope, the external walls have a thermal transmittance of 0.38 $Wm^{-2}K^{-1}$ whilst the value of the overall heat transfer coefficient value of the horizontal partitions is U=0.42 $Wm^{-2}K^{-1}$. All the windows have double-pane glasses with a uniform thermal transmittance of 1.12 $Wm^{-2}K^{-1}$.

All the conditioned rooms are heated and refrigerated by fan-coils except the bathroom, which is heated – in winter only – by a radiator. The water which feeds the fan coils, and in winter the radiator, is stored in a tank, which acts as buffer system to dampen temperature oscillations due to sudden changes in outdoor conditions and to cover peak loads that might occur.

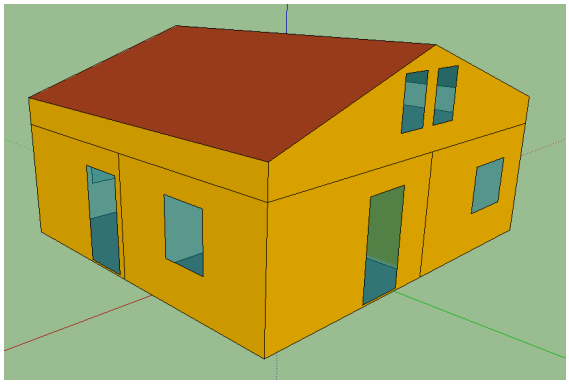

Fig. 1 – Sketch of the building

One water tank, which is shown as two different tanks in the representation in Fig. 2 and in the simulation, contains hot water in winter (HWT) and refrigerated water in summer (CWT). The water tank has a volume of 0.5 m^3 and is connected to the heat pump.

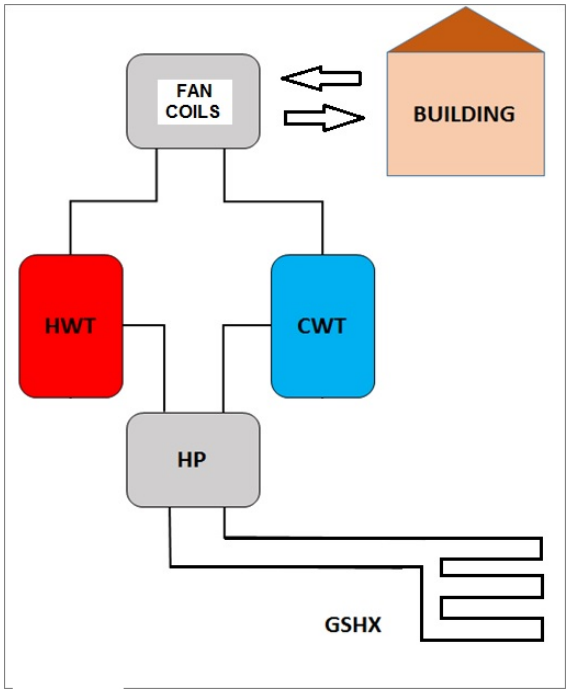

Fig. 2 – Representation of the HVAC system

The heat pump exchanges thermal energy with the ground by means of a horizontal GHE, where a mixture of water and glycol circulates. The geothermal field consists of 5 loops, each 100 m long, of high-density polyethylene pipes 32 mm in diameter

and 2.9 mm thick. The pipes are buried 1.5 m below the surface and are connected in parallel. The wheelbase between the pipes is 0.4 m and the total surface area occupied by the geothermal field is about 180 m².

The nominal cooling power of the heat pump is 1.8 kW with nominal energy efficiency ratio EER=4.5, when the temperature of the fluid at the evaporator is in the 15-10 °C range and the temperature of the fluid at the condenser lies in the 30-35 °C interval; the nominal heating power is 2.4 kW with a coefficient of performance COP=4.0, when the temperatures of the fluid at the evaporator is between 12 and 7 °C and the fluid at the condenser is at 40-45 °C. To better replicate the machine's actual behaviour, the EER and COP curves were deduced from the manufacturer's data.

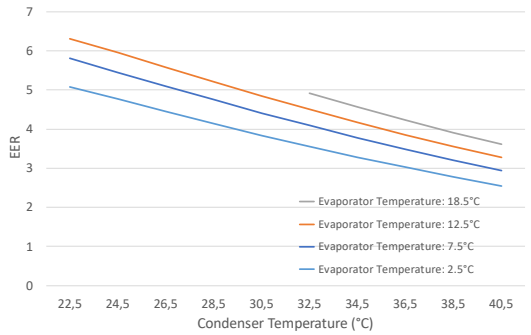

Fig. 3 – EER curves for the heat pump

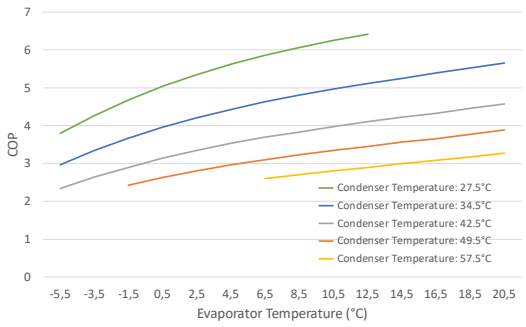

Fig. 4 – COP curves for the heat pump

Fig. 3 shows EER curves versus condenser mean temperature (ΔT=5 K) for different values of the evaporator mean temperature (ΔT=5 K), whilst COP values versus evaporator mean temperature for fixed condenser mean temperatures are plotted in Fig. 4 for the working ranges of interest.

The temperature set points of water feeding the fan coils are 42.5 °C in winter and 8.5 °C in summer, assuming a dead band of ± 2.5 °C (summer) and ± 1.5 °C (winter) for temperature control purposes.

Three different hydraulic circuits are inserted in the model: one to connect the heat pump to the GSHX, another between the HP and the water tank and the last circuit connects the water tank to the fan coils inside the building. The inlet temperature of each component is time dependent, whilst the circuits mass flow rates, when the pumps are switched on, are set at a constant value. The electric power required by the fan coils ranges between 20 and 50 watts, depending on the fan velocity. Two levels of temperature control are employed. The first is at the water tank, as described above, and the second in each single room.

During winter, the temperature in each room of the building is set at 20 °C (bathroom 22°C), whilst in summer it is at 26 °C, except the bathroom where cooling is not required. Weather data for the city of Rome were obtained from the Meteonorm database, included in the Trnsys® package.

The simulations were run at time steps of 5 minutes over the whole year, spanning both the heating and cooling seasons. The most significant data obtained and the quantities derived from them are discussed in the following section.

3. Analysis and Discussion of the Results

The COP and EER of the GCHP, both defined as the ratio between the energy exchanged with the water tank and the electrical energy supplied to the heat pump were computed over the corresponding seasons.

Fig. 5 shows the COP of the GCHP from the month of November until the end of March.

It is clear that the COP dropped from 4.6-5.2 at the beginning of the winter season to 3.8-4.4 in the month of January. This was due to the temperature depletion of the ground and, of course, to the harsher external conditions. It remained on this range until the middle of March and rose during the last days of the heating season. A similar behaviour can be observed analysing the energy efficiency ratio during the summer season. Fig. 6 shows the EER of the GCHP for three most important months in the

summer. In the beginning, the EER stayed in the range of 4.1-4.4, then it dropped down to 3.0-3.4 at the end of the summer season. In this case, the lowest values obtained were for the month of August, when outdoor temperatures were at their highest, and the ground had experienced a continuous temperature increase owing to contributions from both the GHE and solar radiation.

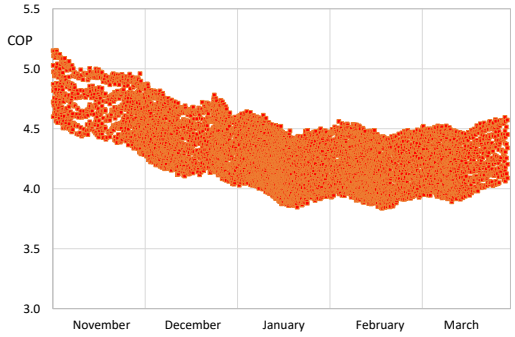

Fig. 5 – Winter season COP for the GCHP

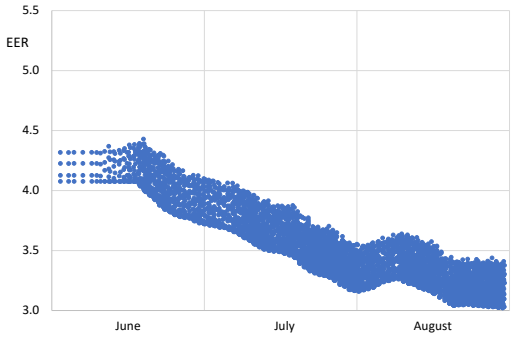

Fig. 6 – Summer season EER for the GCHP

Further, the heating monthly performance factor (HMPF) of the whole HVAC-Building system (adaption form Dincer, 2017) was calculated on a monthly basis as:

$$\mathrm{HMPF} = \frac{Q_{bu}}{W_{el}} \qquad (1)$$

Where Q_{bu} (J) is the energy delivered in a month to the rooms of the building by the HVAC to keep the desired set-point conditions and W_{el} (J) is the electric energy consumption during the same period, considering both the GSHP and all auxiliaries (fans, pumps, etc.).

Monthly Energy Efficiency Ratio (MEER, again, adapted from Dincer, 2017) is computed in the same way as the HMPF, albeit for the summer months, as shown in Equation (2):

$$\mathrm{MEER} = \frac{Q_{bu}}{W_{el}} \qquad (2)$$

Both HMPF and MEER define the behaviour of the HVAC-Building assembly in terms of firs-law analysis, and the results are shown in Fig. 7.

The heating and cooling system coupled with the GCHP exhibits an excellent control of temperature and high-performance parameters (HMPF and MEER), as shown in Fig. 7.

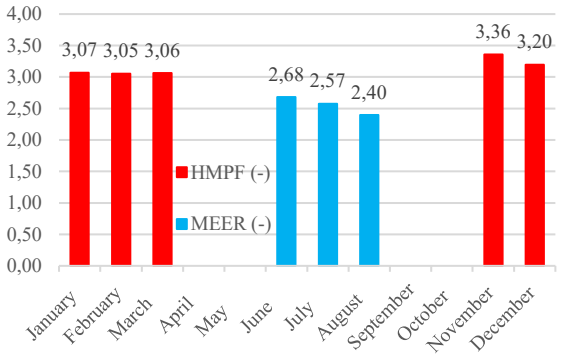

Fig. 7 – HMPF (red) and MEER (blue) for the combined system

The HMPF of the whole system from the month of November until the end of March decreased from 3.36 at the beginning of the winter season to 3.07 in the month of January. At the beginning of the summer season the MEER averaged 2.68; it then decreased to 2.40 at the end of the summer season. Although both HMPF and SEER could be shown and analysed in their evolution during some typical winter and summer days, this would be of little significance, and would in fact be misleading, because the disturbances (variable outdoor conditions and thermal loads) and system response are decoupled thanks to the presence of water storage tanks. Indeed, their purpose is to offer a thermal energy buffer to increase the efficiency of the system, possibly using advanced control strategies (D'Ettorre et al., 2019).

An exergy analysis has also been carried out both at system and component level. For the whole system the overall exergy efficiency ζ has been calculated for each month as:

$$\zeta = \frac{Ex_{bu}}{W_{el}} \qquad (3)$$

Where Ex_{bu} is the total exergy in joule delivered to the building in a month and obtained as the summation of the amount of exergy delivered to the room

in the building. Its value was computed as:

$$\sum_{i=1}^{n} Q_{r,i} \cdot \left(1 - \frac{T_0}{T_{r,i}}\right) = \sum_{i=1}^{n} Q_{r,i} \cdot \eta_C \left(\frac{T_0}{T_{r,i}}\right) \quad (4)$$

In Equation (4), $Q_{r,i}$ is the energy delivered to the i-th room, which is at temperature $T_{r,i}$ (K), and T_0 (K) is the temperature of the dead state, which corresponds to the outdoor temperature, η_C is the Carnot factor, and n is the number of rooms.

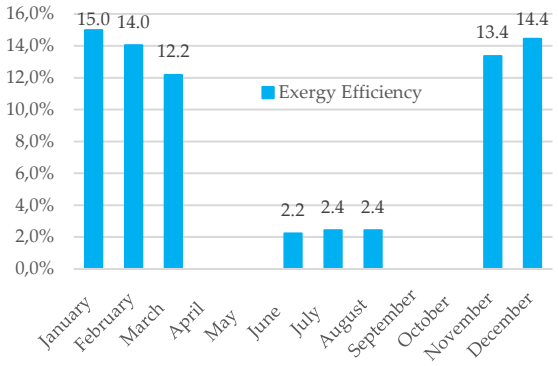

Fig. 8 – Monthly overall exergy efficiency (%) for the system

The reference temperature is chosen as time-dependent on the account of it also being the disturbance to the thermal system (HVAC-building), which therefore determines its behaviour over time and also represents the instant thermodynamic condition at which no useful work may be extracted from any system interacting with the environment. Choosing a fixed state, i.e. the minimum value recorded over each season, would be of no technical significance, since the temperature difference would amount to a few kelvins, and furthermore, the instant energy demands of the building are not dictated by such harsh conditions. If comparison between the exergy performance of the present system and another (e.g. an air-source heat pump) is desired, the same outdoor temperature history should be adopted for both cases, which is consistent with the present choice and makes any issues related to an 'absolute state', such as that given by some reference temperature a moot point. The results are shown in Fig. 8.

The results of the monthly exergy efficiency align with those expected for this kind of system (Verda et al., 2016); it is, however, interesting to note that the highest efficiencies during winter heating were obtained for the coldest months (December and January). This trend was also replicated for the summer, when August is the month with the best performance. It can be noted how exergy efficiency had a maximum (around 15%) in the middle of the winter season (January). Indeed, in this period the heating demand of the building and the Carnot efficiency associated with the heat transferred to the rooms reached their peak. The use of the ground as a heat source makes it possible to better exploit the energy resource in the coldest days. During the summer, the exergy efficiency dropped to values significantly lower than those obtained in winter: in particular, it lies between 2.2% and 2.4%. This is due to the very low values of the Carnot efficiency; during this time, the temperature of the rooms (which is kept at a set-point value of 26 °C) was close to T_0, and the Carnot efficiency therefore dropped to very low values approaching zero.

This behavior can be explained by observing the amount of exergy extracted from the ground by the GHEs, Ex_g (J), which is calculated on a monthly basis using Equation (5):

$$Ex_{gd} = \sum_{j=1}^{n} \dot{m}_{w,gd,j} \cdot \left(h_{w,gd,,o} - h_{w,gd,i} - T_0 \cdot c \cdot \ln\left(\frac{T_{w,gd,o}}{T_{w,gd,i}}\right)\right)_j \Delta\tau \quad (5)$$

Where $\dot{m}_w$ is the water mass flowrate (kg s^{-1}) through the GHE over the time interval $\Delta\tau$ (s) , c is the specific thermal capacity (kJ kg^{-1} K^{-1}), n is the number of time intervals over the period considered, $h_{w,o}$ and $h_{w,i}$ the outlet and inlet specific enthalpies (kJ kg^{-1}) of the water, and $T_{w,o}$ and $T_{w,i}$ (K) the outlet and inlet temperatures, respectively. The results are plotted in Fig. 9: it is evident that the maximum amount of exergy yield is obtained in the month with extremes of either heat or cold.

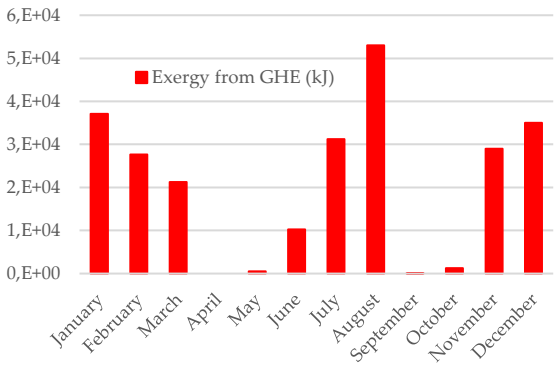

Fig. 9 – Monthly exergy extraction from GHE

Despite the amount of exergy extracted from the ground, the GHE is the component with the lowest exergy efficiency, which is similar to that of the whole system, as shown in Fig. 10.

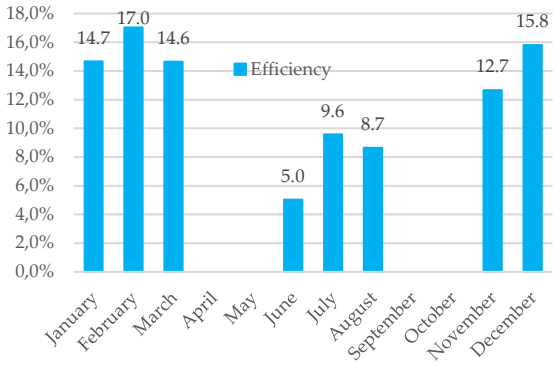

Fig. 10 – Monthly efficiency (%) for GHE

The explanation for this behaviour is to be sought in the way the exergy efficiency is defined for the component, Equation (6):

$$\zeta_{GH} = \frac{Q_{gh} \cdot \eta_C\left(\frac{T_0}{T_{lm,gh}}\right)}{Q_{gh} \cdot \eta_C\left(\frac{T_0}{T_g}\right)} = \frac{T_{lm,gh} - T_0}{T_g - T_0} \frac{T_g}{T_{lm,gh}} \quad (6)$$

$T_{lm,gh}$, (K) is the log-mean temperature difference between outlet and inlet of the GHE, whilst $T_{g.}$, (K), is the ground temperature, which should be uniform. The second rate in Equation (6) is close to unity, but the first is very small most of the time, hence the limited exergy efficiency.

The heat pump, on the other hand, has a different behaviour. In particular, its exergy efficiency is calculated as:

$$\zeta_{HP} = \frac{Ex_{ld}}{W_{el,hp} + Ex_{gh}} \quad (7)$$

Where Ex_{ld} (J) is the exergy that the heat pump supplies to the two storage tanks, Ex_{gh} (J) is the exergy which the pump receives from the ground through the heat exchanger and $W_{el,hp}$ (J) is the energy required to power the heat pump. The two contributions are obtained from Equations (8) and (9):

$$Ex_{ld} = \sum_{j=1}^{n} \dot{m}_{w,ld,j} \cdot \left(h_{w,ld,o} - h_{w,ld,i} - T_0 \cdot \cdot c \cdot \ln\left(\frac{T_{w,ld,o}}{T_{w,ld,i}}\right)\right)_j \Delta\tau \quad (8)$$

and

$$Ex_{gh} = \sum_{j=1}^{n} \dot{m}_{w,gh,j} \cdot \left(h_{w,gh,o} - h_{w,gh,i} - T_0 \cdot \cdot c \cdot \ln\left(\frac{T_{w,gh,o}}{T_{w,gh,i}}\right)\right)_j \Delta\tau \quad (9)$$

The symbols are analogous to those in Equation (5), but it must be remarked that if $\dot{m}_{w,gh,j}$ is the same as $\dot{m}_{w,gd,j}$, this is not the case for the values of the enthalpies nor of the water temperatures appearing in Equation (5) and in Equation (9), respectively.

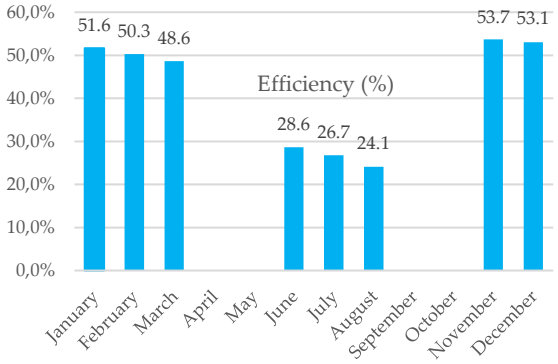

Fig. 11 – Monthly exergy efficiency (%) for the heat pump

The monthly exergy efficiencies for the heat pump are shown in Fig. 11. In can be noted that the trend is constantly diminishing, which hints at a steady decrease in the potential of the ground to supply exergy. This is due to the constant thermal depletion of the ground (which is progressively cooled in winter and heated in summer); this trend is enhanced by the type of GHE loops, which are laid less than 2 metres below the ground level and are therefore more influenced by thermal losses/gains from ambient temperature and radiation. It must also be noted, however, that this is an intrinsic characteristic of the model adopted to simulate the ground temperature, T_{gd} (K), (Kusuda et al., 1965).

The yearly exergy efficiency for one of the bedrooms, which is representative of the behaviour of the other rooms too, is shown in Fig. 12.

The efficiency is calculated as:

$$\zeta_{HP} = \frac{Ex_r}{W_{el,fc} + \Delta Ex_{fc}} \quad (10)$$

Ex_r (J) is similar to Ex_{bu} in Equation (3), but refers to a single room, $W_{el,hp}$ (J) is the electric energy to power the fan coils and ΔEx_{fc} is the exergy variation of the water flow between inlet and outlet of the fan coil.

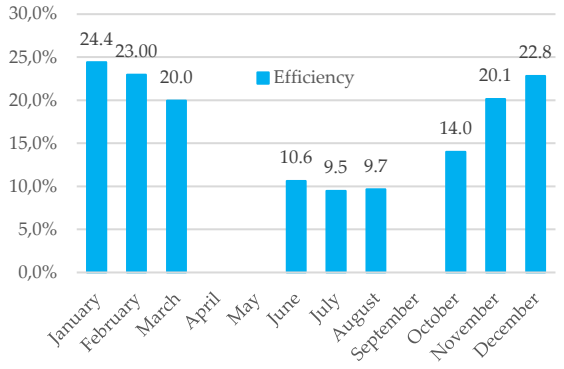

Fig. 12 – Monthly exergy efficiency (%) for one bedroom

ΔEx_{fc} is computed as per Equation (11), with the symbols denoting the same quantities as in Equations (8) and (9), except that they refer to the water flowing through the fan coils.

$$\Delta Ex_{fc} = \sum_{j=1}^{n} \dot{m}_{w,fc,j} \cdot \left(h_{w,fc,o} - h_{w,fc,i} - T_0 \cdot c \cdot \ln\left(\frac{T_{w,fc,o}}{T_{w,fc,i}}\right)\right)_j \Delta\tau \quad (11)$$

The maximum exergy efficiency is for the coldest months, both in winter (December to February) and in summer (June). In this case, the electric demand of the fan coils is likely to determine this trend.

4. Conclusions

This work presents a first- and second-law analysis of the yearly performance of a HVAC system coupled with a ground-source heat pump, used to control the temperature in a single-family dwelling located in Rome.

The results showed excellent energy performance of the system both in the cooling and heating periods. Exergy efficiencies are markedly lower during the summer owing to the lower Carnot efficiencies. The analysis at component level also highlighted the GSHX to be the least-efficient component.

Future developments of the research include a comparison, for the same building, between the HVAC system presented here (GSHP) and different kinds of generation systems such as a traditional gas-fired boiler or an air source heat pump.

Nomenclature

Symbols

c	Specific capacity (kJ kg^{-1} K^{-1})
COP	Coefficient of performance (-)
EER	Energy efficiency ratio (-)
h	Specific enthalpy (kJ kg^{-1})
HMPF	Heating Monthly Performance Factor (-)
$\dot{m}$	Mass flowrate (kg s^{-1})
Q	Thermal energy (J)
SEER	Season Energy Efficiency Ratio (-)
T	Temperature (K)
U	Overall heat transfer coefficient (Wm^{-2}K^{-1})
W	Work (J)
$\Delta\tau$	Time interval (s)
η	Carnot factor (-)
ζ	Exergy efficiency (-)

Subscripts/Superscripts

bu	building
el	electric
fc	fan coil
gd	ground
gh	ground heat exchanger
HP	Heat pump
i	inlet
ld	load
lm	log-mean
o	outlet
r	room
w	water
0	ambient (dead state)

References

D'Ettorre, F., P. Conti, E. Schito, D. Testi. 2019. "Model predictive control of a hybrid heat pump system and impact of the prediction horizon on cost-saving potential and optimal storage capacity." *Applied Thermal Engineering* 148: 524-535.

Dincer, I. 2017. *Refrigeration Systems and Applications.* John Wiley & Sons.

European Parliament and of the Council. 2009. "Directive 2009/28/EC of the European Parliament and of the Council of 23 April 2009 on the promotion of the use of energy from renewable sources and amending and subsequently repealing Directives 2001/77/EC and 2003/30/EC." *Official Journal of the European Union.*

European Parliament and of the Council. 2018. "Directive (EU) 2018/844 of the European Parliament and of the Council of 30 May 2018 amending Directive 2010/31/EU on the Energy Performance of buildings and Directive 2012/27/EU on Energy Efficiency." *Official Journal of the European Union* 19.6.2018.

European Parliament and Council. 2018. "Directive (EU) 2018/2001 of the European Parliament and of the Council of 11 December 2018 on the promotion of the use of energy from renewable sources." *Official Journal of the European Union.*

Evola, G., V. Costanzo, L. Marletta. 2018. "Exergy Analysis of Energy Systems in Buildings." *Buildings* 8(12), 180.

Klein, S.A., et al. 2010. *TRNSYS Version 17.* Madison, U.S.A.: Solar Energy Laboratory, University of Wisconsin-Madison.

Kusuda, T., P.R. Achenbach. 1965. "Earth Temperature and Thermal Diffusivity at Selected Stations in the United States." *ASHRAE Transaction* 71(1): 61–75.

Loreti, L., P. Valdiserri, M. Garai, 2016. "Dynamic Simulation on Energy Performance of a School." *Energy Procedia* 101: 1026–1033.

Lucchi, M., M. Lorenzini, P. Valdiserri. 2017. "Energy performance of a ventilation system for a block of apartments with a ground source heat pump as generation system." *Journal of Physics: Conference Series* 796(1).

Sanaye, S., B. Niroomand. 2010. "Horizontal ground coupled heat pump: Thermal-economic modeling and optimization." *Energy Conversion and Management* 51: 2600–2612.

Sarbu, I., C. Sebarchievici. 2014. "General review of ground-source heat pump systems for heating and cooling of buildings." *Energy and Buildings* 70: 441–454.

Serova, E. N., V. M. Brodianski. 2004 "The concept ''environment'' in exergy analysis. Some special cases." *Energy* 29: 2397–2401.

Valdiserri, P. 2018. "Evaluation and control of thermal losses and solar fraction in a hot water solar system." *International Journal of Low Carbon Technologies* 13: 260–265.

Verda, V., S. Cosentino, S. Lo Russo, A. Sciacovelli. 2016. "Second law analysis of horizontal geothermal heat pump systems." *Energy and Buildings* 124: 236–240.

Zhou, Y., G. Gong. 2013. "Exergy analysis of the building heating and cooling system from the power plant to the building envelop with hourly variable reference state." *Energy and Buildings* 56: 94–99.